

Intrinsic Piezobirefringence in GaSb, InAs, and InSb†

Peter Y. Yu, M. Cardona,* and F. H. Pollak

Physics Department, Brown University, Providence, Rhode Island 02912

(Received 26 August 1970)

The intrinsic piezobirefringence in InAs, GaSb, and InSb has been measured at room temperature with uniaxial stresses along the [001] and [111] directions. The experimental results were fitted with a theoretical expression involving two adjustable parameters. From one of the parameters, the shear deformation potentials b and d of the valence band edge were obtained. The results are compared with those obtained by other methods. The long-wavelength piezobirefringence is discussed in the light of Phillips's theory of the dielectric constant. A quadratic dependence of the piezobirefringence on stress was observed in the vicinity of the absorption edge, especially for GaSb. This nonlinear effect can be theoretically interpreted without any adjustable parameters. The possibilities of obtaining phase matching in second-harmonic generation with InAs and GaSb by uniaxial stress using a CO₂ laser are also discussed.

I. INTRODUCTION

The stress-induced birefringence due to inter-band transitions (intrinsic piezobirefringence, intrinsic PB) can be measured very accurately in high-purity semiconductors below the fundamental absorption edge.¹⁻³ The PB coefficient usually exhibits considerable dispersion when a direct absorption edge is approached.^{1,3} In this respect most semiconductors fall into three categories: (i) Materials whose absorption edge is direct (e.g., GaAs¹, InSb, InAs, and GaSb) show strong dispersion in the PB coefficient, when this edge is approached. (ii) Materials with a lowest indirect edge and an allowed direct edge at only slightly higher energy (e.g., Ge¹) also exhibit considerable dispersion in the PB coefficient as the indirect edge is approached. (iii) Materials with a lowest indirect edge and direct edges only at much higher energies (e.g., Si¹ and AlSb²) show little dispersion in the PB coefficient as the indirect edge is approached. The interpretation of the shape of the dispersion in the PB coefficient provides a good testing ground for our knowledge of band structures in relationship to optical properties and of the effect of stress on energy bands.

Gavini and Cardona³ explained the dispersion in the PB coefficient of a series of alkali halides as due to the splitting of the valence band edge by stress; they obtained from these measurements the shear deformation potentials of this band edge. For semiconductors Higginbotham *et al.*¹ and Shileika *et al.*² succeeded in explaining the dispersion in the PB coefficient of Ge, Si, GaAs, and AlSb with a model consisting of a series of parabolic bands with edges at the E_0 , $E_0 + \Delta_0$, E_1 , and $E_1 + \Delta_1$ optical gaps and one single oscillator at the E_2 gap. Several related models to interpret the intrinsic PB have also been given by Riskaer and Balslev⁴ and by Wemple and DiDomenico.⁵ In the

present work we apply the theory of Higginbotham *et al.*¹ to three other zinc-blende-type semiconductors, i.e., GaSb, InAs, and InSb. These materials belong to the category (i) listed above: The lowest gap E_0 is direct and allowed. Moreover, the E_1 , $E_1 + \Delta_1$ and other higher gaps are sufficiently far away from the E_0 and $E_0 + \Delta_0$ gaps that they do not contribute to the observed dispersion. As a result we have been able to extract the contributions of E_0 and $E_0 + \Delta_0$ and obtain from them the shear deformation potentials b and d . The long-wavelength or nondispersive contribution of all the higher gaps to the PB coefficient has been explained, at least qualitatively with the simple one-isotropic-band-gap model due to Penn.^{6,7}

The experimental method and the PB results for GaSb, InAs, and InSb at room temperature are described in Sec. II. In Sec. III we discuss the theoretical interpretation of the results, involving the dispersion in the linear PB coefficient due to the lowest direct edges E_0 and $E_0 + \Delta_0$, the quadratic dependence of the PB on stress in the vicinity of E_0 , the possible use of the dispersion in the PB coefficient near E_0 to determine the deformation potentials, and the application of the Penn model to the interpretation of the nondispersive component of the PB coefficient due to the higher gaps. Recently, interest in PB has been promoted by the possibility of using it to produce phase matching in second-harmonic generation (SHG)⁸ and to modulate laser beams acoustically.⁹ The enhancement of phase matching in SHG with InAs and GaSb by application of an uniaxial stress is discussed in Sec. IV.

II. PIEZOBIREFRINGENCE: EXPERIMENTAL SETUP AND RESULTS

The experimental setup used for the study of PB has already been described in detail in the literature^{1,3,10} and will not be reproduced here. Changes

necessary for infrared measurements included the use of a PbS cell cooled to liquid-nitrogen temperature for wavelengths shorter than 4.5μ and a thermocouple for longer wavelengths. For wavelengths longer than 2μ , a pair of gold-wire-grid polarizers¹¹ were used. In order to eliminate the effect of free carriers, samples were chosen to have carrier concentrations below 10^{16} cm^{-3} . In the case of InSb only n -type materials were used since p -type InSb has a much higher absorption below the fundamental gap.¹²

The linear PB coefficient α is obtained by making a least-squares fit of $\epsilon_{\parallel} - \epsilon_{\perp}$, the difference in dielectric constants parallel and perpendicular to the stress axis, to the expression $\alpha X + \beta X^2$, where X is the applied stress with the standard convention that compressive stresses are negative. The values of α for GaSb, InAs, and InSb, measured at room temperature, are shown in Figs. 1, 2, and 3 as a function of reduced frequency.

In all three materials the linear PB coefficient for both [001] and [111] stresses shows considerable dispersion near the absorption edge. It is observed that the sign of the coefficient for GaSb changes from positive to negative near the absorption edge for [001] stress. The results for [111] stress indicate that the same thing would happen if one could get close enough to the edge. Such sign reversal of the linear PB coefficient has also been observed in Ge and GaAs for a [001] stress.¹ For both InAs and InSb the PB coefficient remains negative throughout the wavelength region of our measurements. A feature common to Ge, GaAs, GaSb, InAs, and InSb, is that the linear PB coefficient for the [111] stress is larger than the PB coefficient for the [001] stress at the same wavelength.

III. THEORY

A. Effects Linear in Stress

To explain the observed dispersion in the linear

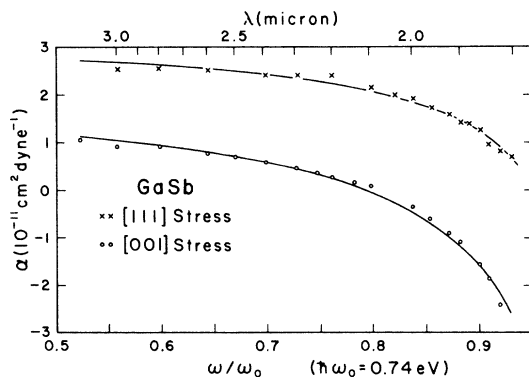


FIG. 1. Linear PB coefficients of GaSb at room temperature as a function of reduced frequency.

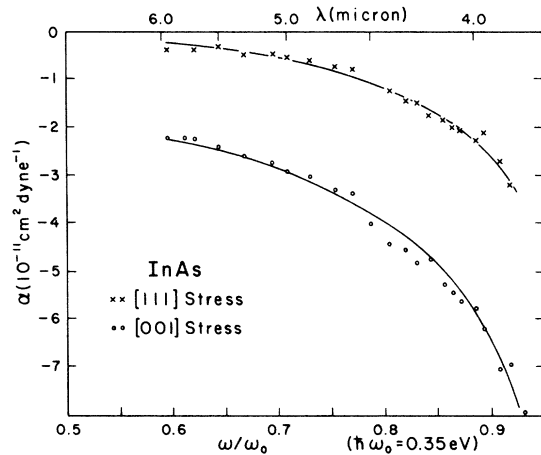


FIG. 2. Linear PB coefficients of InAs at room temperature as a function of reduced frequency.

PB coefficient, we use the parabolic-band model discussed in detail by Higginbotham *et al.*¹ These authors assumed that the band structure of a semiconductor of the germanium-zinc-blende family consists of a number of parabolic bands with the band edges at the E_0 , $E_0 + \Delta_0$, E_1 , and $E_1 + \Delta_1$ optical gaps. The effect of the E_2 gap is included by introducing a simple harmonic oscillator with the resonance energy equal to that of the E_2 gap. The contribution of each band to the linear PB coefficient shows an infinite singularity at the band edge but approaches a constant at photon energies much smaller than the band gap. In the semiconductors we are considering the lowest gaps E_0 and $E_0 + \Delta_0$ are so much smaller than the higher gaps ($3E_0 \approx E_1$ in GaSb, $7E_0 \approx E_1$ in InAs, and $10E_0 \approx E_1$ in InSb) that their contributions in the photon energy

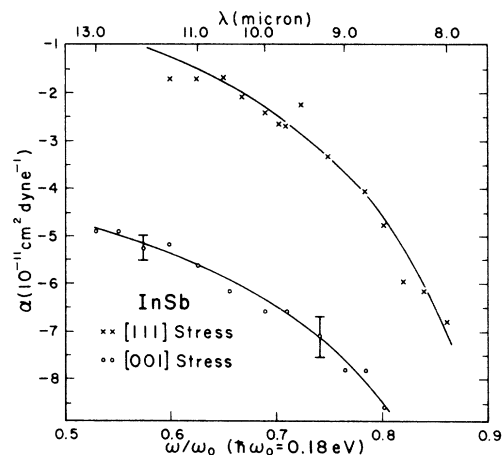


FIG. 3. Linear PB coefficients of InSb at room temperature as a function of reduced frequency.

region of interest (i. e., photon energies smaller than E_0) are practically constant. Thus the dispersion centers we need to consider are only E_0 and $E_0 + \Delta_0$; the model we shall use consists of only four parabolic bands as shown in Fig. 4. The theoretical expressions we obtained for the linear PB coefficients for a [001] stress are (atomic units, e. g., $e = \hbar = m = 1$, will be used throughout this paper unless otherwise specified)

$$\text{(InAs, GaSb)} \quad \alpha = C \left\{ -g\left(\frac{\omega}{\omega_0}\right) + 4f\left(\frac{\omega}{\omega_0}\right) - 4\left(\frac{\omega}{\omega_{0s}}\right)^{3/2} \left[f\left(\frac{\omega}{\omega_{0s}}\right) \right] \right\} + D, \quad (1)$$

$$\text{(InSb)} \quad \alpha = C \left\{ -g\left(\frac{\omega}{\omega_0}\right) + \frac{\omega_0}{\Delta_0} \left[3f\left(\frac{\omega}{\omega_0}\right) \right] \right\} + D. \quad (2)$$

In the above equations $\hbar\omega_0$ and $\hbar\omega_{0s}$ are the energies of the E_0 and $E_0 + \Delta_0$ gaps, respectively, and Δ_0 is the spin-orbit splitting of the top valence bands at the Γ point of the Brillouin zone. $g(x)$ and $f(x)$ are functions defined by

$$f(x) = x^{-2} [2 - (1-x)^{1/2} - (1+x)^{1/2}], \quad (3)$$

$$g(x) = x^{-2} [2 - (1-x)^{-1/2} - (1+x)^{-1/2}]. \quad (4)$$

In deriving Eqs. (1) and (2) we have made use of the fact that for InSb $\omega_{0s} \approx 5\omega_0$ and for InAs and GaSb $\omega_{0s} \approx 2\omega_0$.

The parameter D includes the nondispersive contributions from all the higher gaps to the linear PB coefficient below E_0 . Equations (1) and (2) are

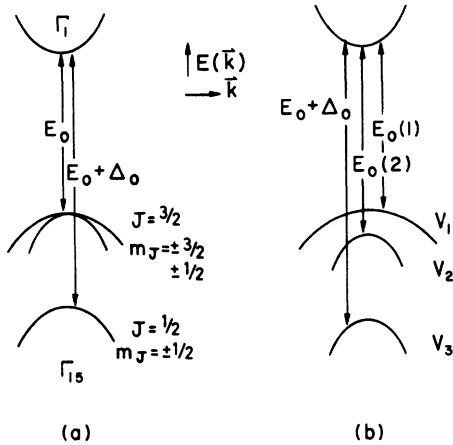


FIG. 4. Four parabolic bands model used in this paper to interpret the dispersion of the PB of GaSb, InAs, and InSb: (a) without stress, (b) with stress. The notation is that of Ref. 1.

also valid for a [111] stress provided C and D are replaced by two new constants C' and D' . The parameters C and C' can be related to the deformation potentials of the E_0 gap by the following expressions:

$$C = \sqrt{2} P^2 (m_0^*)^{3/2} \omega_0^{-5/2} b (S_{11} - S_{12}), \quad [100] \quad (5)$$

$$C' = \sqrt{2} P^2 (m_0^*)^{3/2} \omega_0^{-5/2} \frac{d S_{44}}{2\sqrt{3}}, \quad [111] \quad (6)$$

where b and d are, respectively, the [100] and [111] shear deformation potentials of the valence band at Γ ,

P = matrix element between the top valence band and the lowest conduction band as defined in Ref. 13,

$$m_0^* = \text{joint density-of-states mass} \quad (7)$$

$$= \begin{cases} 0.75 \\ 0.68 \end{cases} \text{ times the effective mass of the lowest conduction band of } \begin{cases} \text{(GaSb, InAs)} \\ \text{(InSb)}, \end{cases}$$

and S_{11} , S_{12} , and S_{44} are the elastic compliance constants.

A least-squares fit to the experimental results was made using Eqs. (1) and (2) with C , C' , D , and D' as adjustable parameters. The values of C , C' , D , and D' obtained in this way are listed in Table I. Some of the constants for the three materials relevant to our calculations are listed in Table II.

1. Deformation Potentials by PB Measurements

From the values of C and C' obtained by fitting the experimental results we can calculate the deformation potentials b and d using Eqs. (5) and (6) and the parameters of Table II. In Table III we have listed the values of b and d for five group IV and III-V semiconductors obtained from PB measurements as compared with the values obtained by other methods.

In the case of GaSb the values obtained by piezoemission and modulated piezoreflectance differ rather widely. Large discrepancies between the deformation potentials measured by PB and modu-

TABLE I. Parameters C , C' , D and D' obtained from a least-squares fit of the experimental PB curves of GaSb, InAs, and InSb shown in Figs. 1, 2 and 3. Their uncertainties are estimated to be $\pm 5\%$ for GaSb, $\pm 7\%$ for InAs, and $\pm 10\%$ for InSb, respectively.

	[001] stress		[111] stress	
	C	D	C'	D'
	$(10^{-11} \frac{\text{cm}^2}{\text{dyne}})$	$(10^{-11} \frac{\text{cm}^2}{\text{dyne}})$	$(10^{-11} \frac{\text{cm}^2}{\text{dyne}})$	$(10^{-11} \frac{\text{cm}^2}{\text{dyne}})$
GaSb	-1.5	+3.6	-0.82	+4.0
InAs	-2.6	+2.1	-1.4	+2.2
InSb	-6.1	+2.0	-6.4	+6.6

TABLE II. Constants used to calculate b and d from the parameters C and C' using Eqs. (5) and (6).

	P^2	m_c	$S_{11} - S_{12}$ $\left(10^{-12} \frac{\text{cm}^2}{\text{dyne}}\right)$	S_{44} $\left(10^{-12} \frac{\text{cm}^2}{\text{dyne}}\right)$	$\hbar\omega_0$ (eV)
GaSb	0.44 ^a	0.047 ^b	2.078 ^c	2.312 ^c	0.74 ^d
InAs	0.38 ^e	0.025 ^d	2.63 ^f	2.526 ^f	0.35 ^d
InSb	0.408 ^g	0.0135 ^d	3.118 ^h	3.256 ^h	0.18 ^d

^aThis value is calculated from the band parameters A , B , and $|C|$ given in R. A. Stradling, Phys. Rev. Letters **20**, 217 (1966).

^bR. Braunstein and E. O. Kane, J. Phys. Chem. Solids **23**, 1423 (1962).

^cH. J. McSkimin, W. L. Bond, G. L. Pearson, and H. J. Hrostowski, Bull. Am. Phys. Soc. **1**, 111 (1956).

^dD. Long, *Energy Band in Semiconductors* (Wiley, New York, 1968). These are room-temperature values.

^eC. R. Pidgeon, D. L. Mitchell, and R. N. Brown, Phys. Rev. **154**, 737 (1967).

^fD. Gerlich, J. Appl. Phys. **34**, 2915 (1963).

^gC. R. Pidgeon and R. N. Brown, Phys. Rev. **146**, 575 (1966). This is the liquid-helium-temperature value.

^hR. F. Potter, Phys. Rev. **103**, 47 (1956).

lated piezoreflectance have also been observed by Gavini and Timusk¹⁴ in the alkali halides. They explained qualitatively the difference as due to the fact that in modulated piezoreflectance one measures the small-stress deformation potentials of the excitons instead of those of the one-electron band edges. It is possible that exciton effects also account for the discrepancy between the large-stress piezoemission and the small-stress modulated piezoreflectance values of b and d for GaSb. In all the semiconductors listed in Table III we find a discrepancy smaller than 50% between the values of b and d obtained by PB and by other methods; the only exceptions are the values of b of GaAs and d of Ge. On the whole we expect a larger error in the case of GaAs, where the effect of the E_1 and E_2 gaps becomes dispersive even below E_0 , and in Ge, where the existence of an indirect gap prevents measurements very close to E_0 . This is even more critical for AlSb² and Si¹ where the indirect gap prevents one from approaching the direct gap close enough to observe its dispersion and thus the deformation potentials b and d cannot be reliably determined.

We also find that one of the two deformation potentials obtained by PB always agrees quite well with values obtained by other methods. This occurs for b in InSb and Ge and for d in GaAs and GaSb. The reason for this is not yet understood.

2. Long-Wavelength PB and the Penn Model

As pointed out earlier the nondispersive long-wavelength PB parameters D and D' include the contributions from the higher-lying gaps E_1 and

$E_1 + \Delta_1$, etc. Long-wavelength dielectric properties of semiconductors have been treated quite successfully by Van Vechten⁷ with the Penn Model, a simple model of an insulator in which an average isotropic gap at the edge of a spherical Brillouin zone is assumed. In particular this model predicts the contribution to the change in $\epsilon(0)$ with hydrostatic stress due to the change in the average gap as given by

$$\Delta\epsilon(0)/\epsilon(0) = 5(\Delta r/r), \quad (8)$$

where r is the nearest-neighbor distance. It is natural to ask whether it is possible to predict D with a modified Penn model. The following generalization of Eq. (8) to the case of an arbitrary stress has been suggested recently¹⁵:

$$\Delta\bar{\epsilon}(0)/\epsilon(0) = 5\bar{e}, \quad (9)$$

where $\bar{\epsilon}$ and \bar{e} are the dielectric and strain tensors, respectively. Using Eq. (9) we obtain the nondispersive component of the long-wavelength PB:

$$D = 5\epsilon(0)(S_{11} - S_{12}), \quad [001] \text{ stress} \quad (10)$$

$$D' = \frac{5}{2}\epsilon(0)S_{44}, \quad [111] \text{ stress} \quad (11)$$

Equations (10) and (11) predict the correct sign for D and D' , but a magnitude which is several times too large. This is not surprising since the contributions of the E_0 , E_1 , and E_2 gaps to the long-wavelength PB do not have the same signs. This sign is negative for E_0 and E_1 but positive for E_2 and they partially compensate each other. This fact has not

TABLE III. Shear deformation potentials b and d for some group IV and group III-V semiconductors obtained by PB as compared to other methods.

	Piezobirefringence		Other methods	
	b (eV)	d (eV)	b (eV)	d (eV)
Ge	-3.0	-2.4	-2.8 ^a -2.6 ^b	-4.95 ^a -4.7 ^b
GaAs	-4.1	-6.0	-1.75 ^a -2.0 ^b	-5.55 ^a -6.0 ^b
GaSb	-3.0	-5.1	-3.3 ^a -2.0 ^c	-8.35 ^a -4.6 ^c
InAs	-1.8	-3.6		
InSb	-1.8	-6.4	-2.0 ^d -2.0 ± 0.15 ^e	-4.9 ^d -5.0 ± 0.5 ^e

^aA. A. Gavini and M Cardona, Phys. Rev. B **1**, 672 (1970).

^bReference 13.

^cC. Benoit à la Guillaume and P. Lavallard, J. Phys. Chem. Solids **31**, 411 (1970).

^dF. H. Pollak and J. Halpern, Bull. Am. Phys. Soc. **14**, 433 (1968).

^eC. Benoit à la Guillaume and P. Lavallard, J. Phys. Soc. Japan Suppl. **21**, 188 (1966).

been considered in the simple Penn model. If we remove the E_1 and $E_1 + \Delta_1$ contributions from the long-wavelength PB the agreement with Eqs. (10) and (11) improves. The column labeled " E_1 removed" in Table IV is obtained from D and D' by removing the E_1 and $E_1 + \Delta_1$ contributions as calculated from Eqs. (12) and (15) in Ref. 1. For InSb we also removed the $E_0 + \Delta_0$ contributions since it was not included in Eq. (2). The " E_1 removed" resultant long-wavelength PB agrees quite well with theory for [111] stress. The corresponding long-wavelength PB for [100] stress is still smaller than the theoretical value by a factor of 2-4. This discrepancy could possibly be improved by refinements in the treatment of the average gap such as using the Heine-Jones model.¹⁶

B. Effects Nonlinear in Stress

A quadratic dependence of birefringence on stress was observed by Higginbotham *et al.*¹ in GaAs and Ge near the fundamental edge. We have also observed this effect in GaSb and InAs. In the case of InSb the intensity of the available light source prevented us from approaching the gap close enough to observe nonlinear effects. Also in InAs the error in the observed nonlinear effect does not allow a meaningful determination of its spectral dependence and hence no attempt was made to compare this effect with theory. The quadratic PB coefficients β of GaSb are shown in Fig. 5. The solid line in the figure is a plot of the theoretical expression calculated with the same four-parabolic-band model. For a [001] stress the nonlinear PB coefficient β is given by

$$\beta = G \left[\left(-\frac{3}{4} + \frac{1}{4} \frac{\delta E_H}{\delta E_{001}} \right) g \left(\frac{\omega}{\omega_0} \right) + \frac{1}{4} \frac{\delta E_H}{\delta E_{001}} h \left(\frac{\omega}{\omega_0} \right) \right]. \quad (12)$$

In Eq. (12) $h(x)$ is the function $x^{-2} [2 - (1-x)^{-3/2} - (1+x)^{-3/2}]$, and the quantity $\delta E_H / \delta E_{001} = a(S_{11} + 2S_{12}) / 2b(S_{11} - S_{12})$ (a is the hydrostatic deformation potential of the E_0 gap) is the ratio of the energy shift caused by the hydrostatic component to the

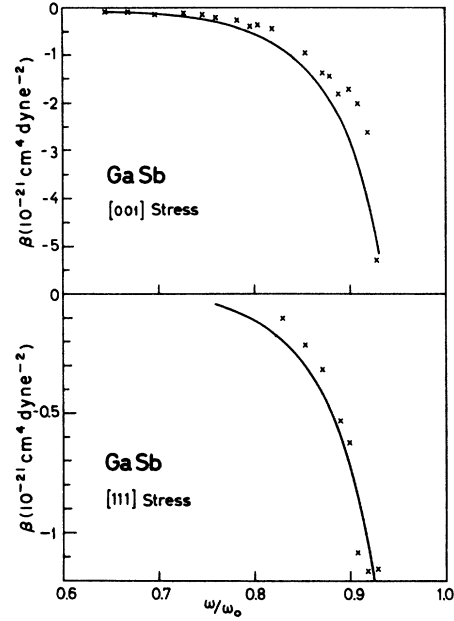


FIG. 5. Nonlinear PB coefficients β of GaSb at room temperature as a function of reduced frequency.

shift caused by the shear component of the stress. For a [111] stress $\delta E_H / \delta E_{001}$ must be replaced by $\delta E_H / \delta E_{111} = a(S_{11} + 2S_{12}) / (d/\sqrt{3}) S_{44}$ in Eq. (12). The constant G is given by

$$G = \begin{cases} 4C b(S_{11} - S_{12}) / \omega_0, & \text{[001] stress,} \\ 2C' d S_{44} / \sqrt{3} \omega_0, & \text{[111] stress} \end{cases} \quad (13)$$

with C and C' defined in Eqs. (5) and (6). The values of G used for the solid curves in Fig. 5 are calculated from the constants C , C' obtained by fitting the linear PB curves. The hydrostatic deformation potential a for GaSb is obtained from the pressure coefficient of the E_0 energy gap.¹⁷

TABLE IV. Nondispersive contributions D and D' to the linear PB from the higher gaps calculated from Eqs. (10) and (11) as compared with experimental results. The column labeled " E_1 removed" is obtained from D and D' by removing the contributions of the E_1 and $E_1 + \Delta_1$ gaps.

	[100] Stress (10^{-11} cm ² /dyne)		[111] Stress (10^{-11} cm ² /dyne)	
	Experiment	Theory (Eq. 10)	Experiment	Theory (Eq. 11)
	D	" E_1 removed"	D'	" E_1 removed"
Ge	1.9 ^a	4.6	3.6 ^a	6.0
GaAs	2.5 ^a	3.6	2.7 ^a	4.2
GaSb	3.6	8.1	4.0	6.0
InAs	2.1	4.7	2.2	3.2
InSb	2.0	5.6	6.6	10.1

^a Obtained from Ref. 1 with the contributions from the E_0 and the $E_0 + \Delta_0$ gaps removed.

No adjustable parameters were used and we note the good agreement between the experimental result and the theoretical prediction. It is worthwhile pointing out that, as shown in Eqs. (12) and (13), the nonlinear effect arises mainly from the combined effect of the hydrostatic and shear components of the uniaxial stress: The hydrostatic increase of the gap under compression produces, as shown in Eqs. (5) and (6), a decrease in the magnitude of the E_0 contribution to the PB.

IV. PHASE MATCHING BY APPLICATION OF UNIAXIAL STRESS

The effect of uniaxial stress on the coherence length (l_{coh}) for second-harmonic generation (SHG) in InAs and GaAs was investigated experimentally by Wynne and Bloembergen⁸ with a 10.6- μ CO₂ laser. The experimental geometry used is shown in Fig. 6(a). In this configuration the change with stress in the refractive index difference of the medium at the first and the second harmonic is given by

$$\Delta[n(2\omega) - n(\omega)] = -\frac{1}{2}[\pi_{11}(2\omega)n_0^3(2\omega) - \pi_{12}(\omega)n_0^3(\omega)]X, \quad (14)$$

where π_{11} , π_{12} are the components of the 4th-rank piezo-optical tensor.¹⁸ The coherence length is related to the refractive-index difference $n(2\omega) - n(\omega)$ by⁸

$$l_{\text{coh}} = \frac{\lambda_0}{4} \frac{1}{n(2\omega) - n(\omega)}. \quad (15)$$

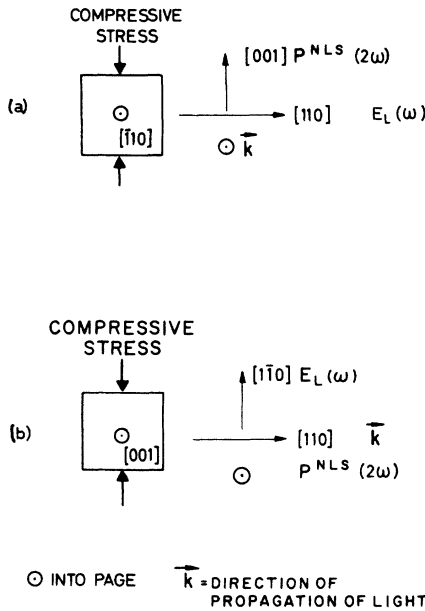


FIG. 6. Possible geometries for producing phase matching in SHG in InAs and GaSb with uniaxial stress (a) [001] stress (b) [110] stress.

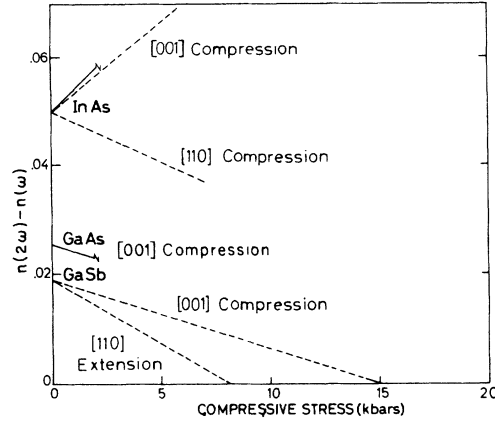


FIG. 7. Variation of the refractive-index difference $\Delta[n(2\omega) - n(\omega)]$ with uniaxial stress. The solid lines are the experimental results of Wynne and Bloembergen taken from Ref. 8. The curves are broken off at the points where the crystals broke. The dashed curves are obtained from our results on the PB of InAs and GaSb.

Thus we can increase l_{coh} if we can reduce $n(2\omega) - n(\omega)$ by applying a uniaxial stress. $\Delta[n(2\omega) - n(\omega)]$ can be related to the linear PB coefficient if both 2ω and ω are far away from the fundamental gap. This is true for InAs and GaSb when a CO₂ laser is used. Under such conditions the dispersion in n , π_{12} , and π_{11} will be small so we can make the following approximations:

$$\Delta[n(2\omega) - n(\omega)] \approx -\frac{1}{2}n_0^3(2\omega)[\pi_{11}(2\omega) - \pi_{12}(2\omega)]X, \quad (16)$$

$$\Delta[n(2\omega) - n(\omega)] \approx (1/2n_0)[\alpha]_{001}X. \quad (17)$$

Thus for a given type of stress (e.g., a compressive one) l_{coh} increases only when $[\alpha]_{001}$ at 2ω is positive. This is what Wynne and Bloembergen observed for GaAs. In InAs, however, they found that l_{coh} decreases with compressive stress; they gave as a possible reason the fact that the second harmonic of the photon energy of the CO₂ laser is close enough to the gap of InAs for the linear PB coefficient to change sign. From our results we found that in InAs the second-harmonic photon energy is sufficiently far from the fundamental gap for the dispersion to be negligible there. In fact, there is no sign reversal in the linear PB of InAs since the contribution of the lowest direct gap to the long-wavelength PB coefficient is large enough to make it negative. The same conclusion is true for InSb. This dominant contribution of E_0 to the PB is responsible for the decrease in l_{coh} observed by Wynne and Bloembergen for InAs.

In order to increase l_{coh} with uniaxial stress in InAs we have to apply a tensile [001] stress or a compressive [110] stress. The geometry for a [110] stress is shown in Fig. 6(b). By arguments

similar to those used in deriving Eq. (17) we conclude that for a [110] stress,

$$\Delta[n(2\omega) - n(\omega)] = (1/4n_0)[\alpha]_{001} + [\alpha]_{111}X. \quad (18)$$

The change in $n(2\omega) - n(\omega)$ with a [110] compressive stress in InAs is shown in Fig. 7 together with the results of Wynne and Bloembergen. The discrepancy between the two results for the [001] compression is about 20%, which is the accuracy claimed by Wynne and Bloembergen. Our result should be accurate to better than 10% for InAs. Also it should be pointed out that we have been able to apply twice the maximum stress they reached without breaking the sample.

Similar results for GaSb are shown also in Fig. 7. Phase matching should be achieved with a [001] compression at 15 kbar. We have been able to compress the crystal up to 5 kbar without crushing it. It is quite possible that cooling the crystal to liquid-nitrogen temperature will further increase its mechanical strength but certainly not up to 15

kbar. A more hopeful case is possibly a [110] extension which should produce phase matching at 8.2 kbar. Wynne and Bloembergen pointed out that one disadvantage of GaSb in SHG is the presence of free-carrier absorption. We believe that cooling a high-purity or compensated crystal to liquid-nitrogen temperature should help to overcome this disadvantage.

ACKNOWLEDGMENTS

We are grateful to Dr. A. Gavini, Dr. J. C. Phillips, and Dr. J. J. Wynne for making available to us copies of their work prior to publication. Helpful discussions with Dr. A. Gavini and Dr. C. W. Higginbotham are also acknowledged. The materials used were obtained from Bell and Howell Inc., Pasadena, Calif. Part of this work was completed when two of the authors (P. Y. Y. and M. C.) were staying at the Deutsches Elektronen-Synchrotron (DESY). They wish to thank members of the group F 41 at DESY for their hospitality. One of the authors (P. Y. Y.) is also indebted to General Telephone and Electronics for a fellowship.

[†]Work supported by the National Science Foundation, and the Army Research Office, Durham.

*J. S. Guggenheim Memorial Foundation Fellow.

¹C. W. Higginbotham, M. Cardona, and F. H. Pollak, *Phys. Rev.* **184**, 821 (1969).

²A. Yu. Shileika, M. Cardona, and F. H. Pollak, *Solid State Commun.* **7**, 1113 (1969).

³A. A. Gavini and M. Cardona, *Phys. Rev.* **177**, 1351 (1969).

⁴S. Riskaer and I. Balslev, *Phys. Letters* **21**, 16 (1966).

⁵S. H. Wemple and M. DiDomenico Jr., *Phys. Rev. B* **1**, 193 (1970).

⁶D. Penn, *Phys. Rev.* **128**, 2093 (1962).

⁷J. A. Van Vechten, *Phys. Rev.* **182**, 891 (1969); **187**, 1007 (1969) and references therein.

⁸J. J. Wynne and N. Bloembergen, *Phys. Rev.* **188**, 1211 (1969).

⁹R. W. Dixon, *J. Appl. Phys.* **38**, 5149 (1967).

¹⁰A. Feldman, *Phys. Rev.* **150**, 748 (1966).

¹¹Perkin Elmer Corp., Norwalk, Conn.

¹²G. W. Gobeli and H. Y. Fan, *Phys. Rev.* **119**, 613 (1960).

¹³F. H. Pollak and M. Cardona, *Phys. Rev.* **172**, 816 (1968).

¹⁴A. A. Gavini and T. Timusk, *Phys. Rev. B* **2**, 2262 (1970).

¹⁵M. Cardona, *J. Res. Natl. Bur. Std.* **74A**, 253 (1970).

¹⁶V. Heine and R. O. Jones, *J. Phys. C* **2**, 719 (1969); P. Y. Yu and M. Cardona, *Phys. Rev. B* **2**, 3187 (1970); J. C. Phillips, *Rev. Mod. Phys.* **42**, 317 (1970).

¹⁷R. Zallen and W. Paul, *Phys. Rev.* **155**, 723 (1967).

¹⁸J. Nye, *Physical Properties of Crystals* (Oxford U. P., Oxford, England, 1957). The relation between the π 's and other piezo-optical constants in the literature is discussed in Ref. 3.